



## In vivo micro-CT imaging of rat brain glioma: A comparison with 3 T MRI and histology

Tobias Engelhorn<sup>a,\*</sup>, Ilker Y. Eyupoglu<sup>b</sup>, Marc A. Schwarz<sup>a</sup>, Marek Karolczak<sup>c</sup>, Holger Bruenner<sup>c</sup>, Tobias Struffert<sup>a</sup>, Willi Kalender<sup>c</sup>, Arnd Doerfler<sup>a</sup>

<sup>a</sup> Department of Neuroradiology, University of Erlangen-Nuremberg, Schwabachanlage 6, D-91054 Erlangen, Germany

<sup>b</sup> Department of Neurosurgery, University of Erlangen-Nuremberg, Germany

<sup>c</sup> Institute of Medical Physics, University of Erlangen-Nuremberg, Germany

### ARTICLE INFO

#### Article history:

Received 12 March 2009

Received in revised form 10 April 2009

Accepted 15 April 2009

#### Keywords:

Glioma

Micro-CT

3 T

MRI

Rat

### ABSTRACT

The aim of this study was to evaluate the potential of a novel micro-CT system to image in vivo the extent of tumor in a rat model of malignant glioma compared to 3 T magnetic resonance imaging (MRI) and histology. Fourteen animals underwent double dose contrast-enhanced imaging with micro-CT and 3 T MRI using a clinical machine at day 10 after stereotactic F98 glioma cell implantation. Calculation of the volume of the contrast-uptaking part of the tumor was done by manually outlining the tumor contours by two experienced neuroradiologists. The micro-CT- and MRI-derived tumor volumes were compared to histology as gold standard (hematoxylin and eosin staining and fluorescence staining). There was high interobserver reliability regarding the tumor volumes (Crombach's  $\alpha > 0.81$ ). Also, there was good correlation of micro-CT- and high-field MRI-derived tumor volumes compared to histology:  $72 \pm 21 \text{ mm}^3$  and  $69 \pm 23 \text{ mm}^3$  compared to  $81 \pm 14 \text{ mm}^3$ , respectively ( $r > 0.76$ ). Both the micro-CT- and MRI-derived tumor volumes were not significantly smaller compared to histology ( $P > 0.14$ ). In conclusion, micro-CT allows in vivo imaging of the contrast-enhancing part of experimental gliomas with an accuracy comparable to high-field MRI.

© 2009 Elsevier Ireland Ltd. All rights reserved.

Although clinical computed tomography (CT) systems can be applied for small animal imaging [15] a variety of scaled-down pre-clinical CT systems have lately been developed to account for the difference in size between humans and small rodents by scaling the scanner parameters to the size of the examined object [17]. Small animal CT systems with spatial resolution below  $500 \mu\text{m}$  (mini- or micro-CT) are commercially available today [12]. Depending on the detector technology used and the required resolution, volume scans with isotropic spatial resolution of approximately  $100 \mu\text{m}$  can be acquired with dedicated micro-CT systems within few minutes [22].

A X-ray exposure below 100 mGy for scanning a whole rat (or below 20 mGy for scanning the skull) makes small animal micro-CT feasible [4]. Although this radiation exposure to animals is one of the biggest disadvantage of micro-CT systems compared to magnetic resonance (MR) scanners, it still offers higher spatial resolution [1]. Besides, in experimental settings with a small number of measurements, radiation exposure can often be neglected.

While functional and metabolic imaging in animals is the domain of positron emission tomography (PET), single photon

emission computed tomography (SPECT) and in part of dedicated small MR scanners with a magnetic field strength mostly greater than 7 T [3], today's clinical whole body 3 T MR scanners show potential for sub-millimeter anatomical imaging when combined with dedicated small animal radiofrequency coils or surface coils offering a robust and cost-efficient tool for imaging animal models to simulate human diseases like brain glioma [5,14]. Furthermore, stable micro-CT systems also offer the opportunity for studies of animal morphology and diseases [21].

Recently, de Crespigny et al. demonstrated, that ex vivo micro-CT imaging of fixed glioma bearing mouse brains results in tumor volumes close to histology [6].

With the increasing importance of small animal imaging in basic science research during the last years, aim of this study was to evaluate the potential of contrast-enhanced in vivo micro-CT to outline malignant gliomas in a rat model. Thus, micro-CT-derived glioma volumes were directly compared to 3 T magnetic resonance imaging (MRI) and histology to scrutinise how accurate this technique is.

The rat glioma cell line F98 (passage 50–70) was established more than 20 years ago by ethylnitrosourea-induced carcinogenesis in CDF Fischer rats. Growth characteristics, cytological and immunohistochemical features of this cell line have been extensively reported [16]. Cells were cultivated in a humidified

\* Corresponding author. Tel.: +49 9131 85 44824; fax: +49 9131 85 36179.  
E-mail address: [tobias.engelhorn@uk-erlangen.de](mailto:tobias.engelhorn@uk-erlangen.de) (T. Engelhorn).

atmosphere at 37 °C and 5% CO<sub>2</sub> in DMEM (Invitrogen, Karlsruhe, Germany) supplemented with 10% fetal calf serum (Biocrom, Berlin, Germany).

F98 glioma cells were transfected with peGFP-N1 (BD Biosciences Clontech, Saint-Germain-en-Laye, France) using Roti-Fect transfection reagent (Roth, Karlsruhe, Germany) according to the manufacturer's protocol. After 48 h of transfection, the cells were fed with fresh medium. Transfected cells were cultured in a selection medium (containing 700 µg G418/ml) for 1 week and subsequently sorted (MoFlo, DakoCytomation, Germany) two times to accelerate selection process.

Animal experiments were done in congruence to the European Union guidelines for the use of laboratory animals. The protocol for animal experimentation was approved by the local government (permission number 54.2531.31-8/06). Fourteen female Fisher rats weighing 150–200 g (Charles River, Sulzfeld, Germany) were anesthetized using intraperitoneal injection [mixture of 70 mg/kg BW ketamine (Pfizer, Karlsruhe, Germany), 15 mg/kg BW xylazine (Bayer, Leverkusen, Germany) and 0.05 mg/kg BW atropine (Braun, Kronberg-Taunus, Germany)] before fixing them in a stereotactic frame (David Kopf Instruments, Bilaney Consultants Düsseldorf, Germany). F98 rat glioma cells in a volume of 5 µl ( $1.5 \times 10^5$ ) were stereotactically implanted with a Hamilton syringe (VWR, Darmstadt, Germany) into the right frontal lobe of the animals (2 mm lateral to bregma, depth 4 mm from dura). 3 T MRI at day 10 after implantation revealed successful tumor growth all animals.

Imaging was done at day 10 after glioma implantation after intraperitoneal injection of ketamine and xylazine as described above. For all examinations, the body temperature was measured and maintained at  $37 \pm 0.5$  °C with a feedback-regulated heating pad. After MRI examination, all animals were immediately transferred to the micro-CT system; e.g. imaging was within a time span of less than 2 h.

Imaging was performed on a 3 T MR scanner unit (TimTrio, Siemens, Erlangen, Germany) with a 40-mm diameter, small field-of-view orbita surface coil as receiver. Scout images were obtained in coronal, axial, and transverse planes to position the slices accurately. Ten coronal T1-weighted slices, each with 1 mm thickness was then positioned on the transverse scout images to cover the tumor (in most cases on 4–5 slices). The T1-weighted images were acquired with a  $512 \times 512$  matrix, field-of-view = 40 mm, repetition time = 507 ms, echo time = 17 ms, and a total scan time of 6 min 42 s. For contrast-enhanced images, each animal received double dose contrast media application with 0.2 mmol/kg body weight (Magnevist, Schering, Berlin, Germany) intravenously 5 min prior to the acquisition of T1-weighted sequences. Analogous to the T1-weighted images, T2-weighted images were acquired with a  $512 \times 512$  matrix, field-of-view = 40 mm, repetition time = 2800 ms, echo time = 96 ms, and a total scan time of 7 min 11 s.

Scans were performed on a dedicated small animal in vivo micro-CT scanner (TomoScope 30s DUO, VAMP GmbH, Erlangen, Germany) with a 40-mm diameter field-of-view and scan volume length of 37 mm. Each scan was done at 40 kV X-ray tube voltage using "Standard Quality" volume scan protocol (5 min scan duration, 150 mGy radiation dose, spatial resolution about 130 µm at noise level of around 25 Hounsfield units (HU)). The images were acquired with a  $512^2$  matrix and reconstructed using 80 µm isotropic voxels and medium smooth kernel that refers to a reconstruction kernel with a standard Hanning window. A typical image volume consisted of 400 slices, with  $400 \times 400$  pixels each. Images were corrected for cupping artefacts (nonuniformity within slice) and calibrated for water (approximately 0 HU).

Each animal received double dose contrast media application with 2 ml/kg body weight (Imeron 400 MCT, Bracco Altana Pharma GmbH, Konstanz, Germany) intravenously approximately 5 min prior to micro-CT acquisition.

Animals were sacrificed and brains were collected for standard histological procedures. Brains were immersion fixed for 2 days using a mixture of 4% paraformaldehyde and 1% glutaraldehyde diluted in distilled water. After rinsing in PBS, brains were stored at 4 °C in 30% sucrose solution for 5 days. For histological analyses, 10 µm thick coronal sections of tissue were prepared using a cryomicrotome (Cryo-Star HM560, MICROM, Waldorf, Germany). Every 25th section was collected for tumor volumetry and was stained with hematoxylin and eosin solution (H&E) and documented by digital imaging.

F98 glioma cells positive GFP were seeded on 12-mm diameter glass cover slips and used at a confluency of 60–70%. The cells were fixed in 4% paraformaldehyde for 20 min. GFP cells were incubated with Alexa Fluor 568 phalloidin (Invitrogen, Karlsruhe, Germany) for 45 min at room temperature to visualize actin. Finally the cells were embedded in mounting medium (DAKO, Hamburg, Germany) and viewed by a confocal laser scanning microscopy (Leica Inverted TCS, Leica Microsystems, Solms, Germany). Fluorescence-labeled tumor cells were analyzed by an Olympus microscope (IX 71) equipped with a TRITC (excitation filter 510–550 nm, emission 590 nm) and FITC (excitation filter 470–490 nm, emission 510–550 nm) narrow band filter and photographed using a CCD camera (F-View II; Soft Imaging System, Münster, Germany).

The tumor masses (H&E-staining and GFP transfected sections) were manually traced on the computer screen, and areas calculated by respective imaging software (AnalySIS, Soft imaging system, Münster, Germany). The total tumor volume has been calculated as the summed area on all measured areas on all H&E stained slices of one animal and results were multiplied with the factor 25. The same procedure has been used for the GFP transfected sections. Due to the analysis of every 10th section, results were multiplied with the factor 10. MR and CT imaging analysis was performed for each rat on coronal slices using Siemens built-in image processing software to outline tumor volume on the contrast-enhanced images. Outlining of the contrast-uptaking tumor part was done manually by eyeballing and tracing the outer border on magnified CT and MRI slices. For calculation of the micro-CT-derived tumor volume, every 10th slice was used (approximately 20 out of 400 slices). The total tumor volume was calculated as the summed area on all contrast-enhanced slices, multiplied by the slice thickness or distance, respectively [10].

As calculation of the histology- and imaging-derived tumor volume was done by two experienced neuroradiologists (results were averaged), internal consistency reliability of the test/interobserver variability was assessed by Cronbach's  $\alpha$ -test.

CT- and MRI-derived tumor volumes were compared to histology and in addition groups 1 and 2 were compared to each other using regression analysis. Statistical significance was calculated using Student's *t*-test (Statview II, Abacus, Cary, NC, USA).

Throughout the surgical preparation with implantation of tumor cells the average body temperature for all animals was  $37.4 \pm 0.6$  °C. Arterial blood gases ( $pO_2 = 106 \pm 22$  mmHg,  $pCO_2 = 36 \pm 7$  mmHg, pH  $7.39 \pm 0.02$ ) and hematocrit ( $42.3 \pm 2.1\%$ ) remained stable. Throughout the MRI and CT examinations, body temperature was  $37.9 \pm 0.8$  °C. There was no statistically significant difference between the two groups ( $P = 0.65$ ).

Fig. 1 shows the calculated tumor volumes according to micro-CT, 3 T MRI and GFP-staining. Fig. 2 shows a typical glioma in the right frontal and parietal lobe revealed by coronal contrast-enhanced micro-CT and MR images and GFP-staining.

Cronbach's  $\alpha$  was  $>0.81$  for calculation of the histology-, micro-CT-, and MRI-derived tumor volume indicating high interobserver reliability.

The MRI-derived tumor volumes at day 10 after implantation was  $72 \pm 21$  mm<sup>3</sup> and the tumor volume according to micro-CT was

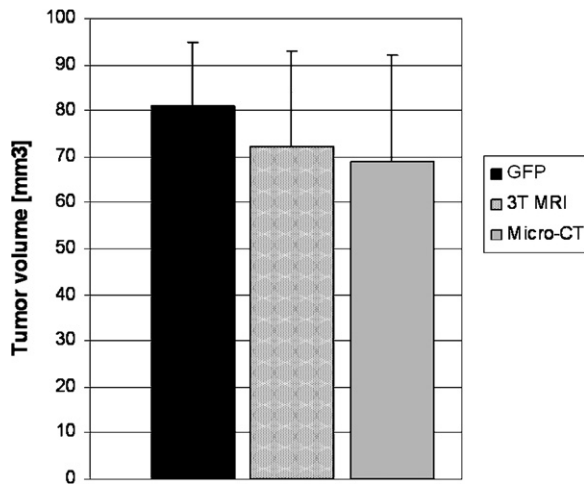


**Fig. 1.** Tumor volumes according to contrast-enhanced 3 T MRI, micro-CT, and GFP-staining at 10 days after glioma cell implantation. Comparing the MRI- and micro-CT-derived tumor volumes to histology, there was no significant difference in tumor volume.

69 ± 23 mm<sup>3</sup>. There was no significant difference between the MRI-derived and the micro-CT-derived tumor volume ( $P > 0.65$ ).

GFP-staining revealed a tumor volume of 81 ± 14 mm<sup>3</sup>, and H&E-staining revealed a slightly higher tumor volume of 82 ± 14 mm<sup>3</sup>, respectively. There was no significant difference in tumor volume according to GFP- and H&E-staining ( $P = 0.91$ ).

If compared the MRI-derived tumor volume to GFP- and H&E-staining, there was no significant difference in tumor volume ( $P = 0.19$  and  $P = 0.17$ , respectively). Additionally, there was no significant difference comparing the micro-CT-derived tumor volume to histology ( $P = 0.18$  and  $P = 0.14$ , respectively).

There was good correlation between the MRI- and micro-CT-derived tumor volumes ( $r = 0.86$ ). Also, there was good correlation between the MRI- and micro-CT-derived tumor volume with histology ( $r > 0.76$ ).

Understanding glioma biology and in particular glioma brain parenchyma interaction still represents a challenge in neurooncological research [2,24]. Nevertheless, tracking glioma progression and analysis of tumor–host interactions are difficult to study with respect to the complex organization of the central nervous system [13]. Thus, in vivo monitoring of brain tumors represents a relevant step in neurooncological studies.

Over the last two decades, modified clinical magnetic resonance imaging systems up to 3 T field strength or specially designed high-field small animal MR-scanners up to 19 T have been established as standard imaging technique to experimentally track glioma growth in vivo [3,9,11,18,23]. In contrast, the clinically well-established computed tomography plays no serious role in detecting brain tumors in experimental settings. Psarros et al. were the first using a

clinical scanner to assess the feasibility of high resolution CT imaging for evaluating experimentally induced brain tumor in rats at days 4–14 after cell implantation [15]. These authors reported a sensitivity and specificity of CT scanning with contrast in detecting tumor bulks of 70% and 100%, respectively. Nevertheless, in 30% of the animals contrast-enhanced CT could not reveal the tumor which was present at autopsy probably due to a lack in spatial resolution.

Within the last years, a variety of scaled-down pre-clinical CT systems have been developed to account for the difference in size between humans and small rodents by scaling the scanner parameters to the size of the examined object [17]. Today, micro-CT systems especially designed to image rodents with spatial resolution below 100 μm are commercially available and can acquire a full brain scan within few minutes [12,22]. While functional and metabolic imaging in laboratory animals is the domain of PET, SPECT and in part of MRI (MR spectroscopy, diffusion tensor imaging, perfusion- and diffusion-weighted imaging), face to face with high-field MRI systems, the spatial resolution achieved with micro-CT is clearly higher. In addition, micro-CT is robust and requires much lower equipment and maintenance costs, which make this technique interesting for experimental tracking of brain tumors in rodents.

Depending on the detector technique used and the X-ray exposure, a big disadvantage of micro-CT compared to conventional clinical scanners is the low soft tissue contrast: our own results and phantom studies indicate that micro-CT is only capable to distinguish lesions having a 30 HU or more difference to the surrounding tissue [22], i.e. micro-CT is only adequate to examine high contrast objects or contrast-uptaking tissue. As limitation in this study, the assessment of the perifocal edema in gliomas was possible with T2-weighted MRI but not with micro-CT. Hence, micro-CT assessment of experimental low-grade gliomas with no or only subtle contrast enhancement – for example the frequently used C6 glioma model – is currently impossible.

Recently, de Crespigny et al. used micro-CT imaging to outline tumors in fixed postmortem mouse brains. Brains were immersion stained in iodinated CT contrast media resulting in clear delineation of tumor margins which closely matched that seen on histology sections [6]. By superimposition of histological slices and corresponding micro-CT slices, these authors demonstrated high correlation between brain tissue and glioma in vivo and ex vivo measurements indicating that tumor volume measurements were not significantly affected by changes in brain tissue ex vivo dimensions.

Besides small animal MR systems, clinical whole body 3 T MR scanners show potential for sub-millimeter anatomical imaging when combined with dedicated small animals radiofrequency coils or commercially available small orbital surface coils [14].

Hence, we evaluated the new technique of micro-CT to in vivo assess experimentally induced highly malignant gliomas in rats compared to a clinical 3 T MRI system with a commercially available orbital surface coil. The imaging-derived tumor volume at day 10 after cell implantation was correlated with histology (fluorescence-

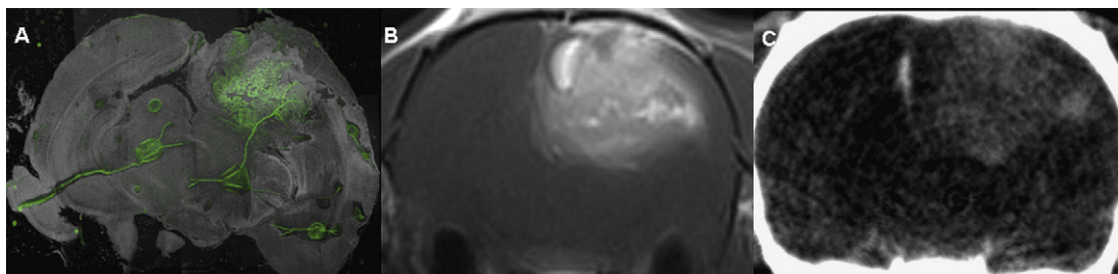


**Fig. 2.** Corresponding coronal GFP-staining (A), contrast-enhanced T1-weighted 3 T MRI (B), and contrast-enhanced micro-CT (C) reveal a large contrast-uptaking glioma in the right frontal and parietal lobe of the animal with midline shift to the left.

labeled tumor cells, hematoxylin and eosin staining) as described recently in detail [20].

In the last years, several MRI studies for brain metastases and brain gliomas demonstrated, that use of double dose contrast media application and delayed imaging results in significantly improved detection rates and better assessment of the contrast-uptaking tumor bulk [20]. Based on our own experimental results the definable micro-CT-derived glioma volume also increases with increasing dosage of CT contrast media (double dose is superior to single dose) and increases additionally with highly iodinated contrast media (we compared Imeron 400 to Imeron 300). Hence, we used double dose Imeron 400 application for micro-CT imaging.

Thereby we could show, that micro-CT imaging reveals the glioma in every animal. The micro-CT-derived contrast-uptaking part of the tumor was slightly but not significantly smaller compared to histology and within the range of the tumor volume assessed with high-field 3T MRI.

With the scan mode chosen (40 kV), contrast-uptaking lesions in the rat brain of less than 0.5 mm diameter could be detected if the high X-ray exposure is of no concern for the specimen as there is an exposure of approximately 150 mGy for 400 slices. As X-ray exposure of the animal might be a limiting factor for longitudinal measurements, the radiation dose can be reduced to approximately 40 mGy without significant loss in spatial resolution and justifiable decrease in signal to noise, which is still compatible with longitudinal studies and below the threshold believed to induce biological effects, e.g. tumor growth, haematopoiesis, bone growth [4].

In conclusion, the new micro-CT systems not only offer the opportunity for quantitative parametric imaging of high contrast structures, e.g. bone density measurements, they also allow in vivo assessment of experimentally implanted gliomas after contrast agent application within the range of a high-field clinical 3T MR system and with good correlation to histology. With further decrease in radiation exposure these systems could become an interesting alternative for longitudinal in vivo monitoring of brain tumors in rodents.

## References

- [1] C.T. Badea, B. Fubara, L.W. Hedlund, G.A. Johnson, 4-D micro-CT of the mouse heart, *Mol. Imaging* 4 (2005) 110–116.
- [2] M.E. Berens, A. Giese, "Those left behind." Biology and oncology of invasive glioma cells, *Neoplasia* 1 (1999) 208–219.
- [3] I. Boehm, F. Traeber, W. Block, H. Schild, Molecular imaging of apoptosis and necrosis—basic principles of cell biology and use in oncology, *Rofo* 178 (2006) 263–271.
- [4] J.M. Boone, O. Velazquez, S.R. Cherry, Small-animal X-ray dose from micro-CT, *Mol. Imaging* 3 (2004) 149–158.
- [5] M.A. Brockmann, S. Ulmer, J. Leppert, R. Nadrowitz, R. Wuestenberg, I. Nolte, D. Petersen, C. Groden, A. Giese, S. Gottschalk, Analysis of mouse brain using a clinical 1.5 T scanner and a standard small loop surface coil, *Brain Res.* 1068 (2006) 138–142.
- [6] A. de Crespigny, H. Bou-Reslan, M.C. Nishimura, H. Phillips, R.A. Carano, H.E. d'Arceuil, 3D micro-CT imaging of post-mortem brain, *J. Neurosci. Methods* 171 (2008) 207–213.
- [9] K. Ikezaki, M. Takahashi, H. Koga, J. Kawai, Z. Kovács, T. Inamura, M. Fukui, Apparent diffusion coefficient (ADC) and magnetization transfer contrast (MTC) mapping of experimental brain tumor, *Acta Neurochir. Suppl.* 70 (1997) 170–172.
- [10] B. Kim, T.L. Chenevert, B.D. Ross, Growth kinetics and treatment response of the intracerebral rat 9L brain tumor model: a quantitative in vivo study using magnetic resonance imaging, *Clin. Cancer Res.* 1 (1995) 643–650.
- [11] P.E. Kish, M. Blaivas, M. Strawderman, K.M. Muraszko, D.A. Ross, B.D. Ross, G. McMahon, Magnetic resonance imaging of ethyl-nitrosourea-induced rat gliomas: a model for experimental therapeutics of low-grade gliomas, *J. Neurooncol.* 53 (2001) 243–257.
- [12] F. Knollmann, R. Valencia, J.H. Buhk, S. Obenauer, Characteristics and applications of a flat panel computer tomography system, *Rofo* 178 (2006) 862–871.
- [13] G.J. Pilkington, R. Bjerkvig, L. de Ridder, P. Kaaijk, In vitro and in vivo models for the study of brain tumour invasion, *Anticancer Res.* 17 (1997) 4107–4109.
- [14] J. Pinkernelle, U. Teichgraber, F. Neumann, L. Lehmkuhl, J. Ricke, R. Scholz, A. Jordan, H. Bruhn, Imaging of single human carcinoma cells in vitro using a clinical whole-body magnetic resonance scanner at 3.0 T, *Magn. Reson. Med.* 53 (2005) 1187–1192.
- [15] T.G. Psarros, B. Mickey, C. Giller, Detection of experimentally induced brain tumors in rats using high resolution computed tomography, *Neurol. Res.* 27 (2005) 57–59.
- [16] G. Reifenberger, T. Bilzer, R.J. Seitz, W. Wechsler, Expression of vimentin and glial fibrillary acidic protein in ethylnitrosourea-induced rat gliomas and glioma cell lines, *Acta Neuropathol.* 78 (1989) 270–282.
- [17] E.L. Ritman, Micro-computed tomography—current status and developments, *Annu. Rev. Biomed. Eng.* 6 (2004) 185–208.
- [18] B.D. Ross, R.J. Higgins, J.E. Boggan, B. Knittel, M. Garwood, 31P NMR spectroscopy of the in vivo metabolism of an intracerebral glioma in the rat, *Magn. Reson. Med.* 6 (1998) 403–417.
- [20] N.E. Savaskan, A. Heckel, E. Hahnen, T. Engelhorn, A. Doerfler, O. Ganslandt, C. Nimsky, M. Buchfelder, I.Y. Eyuepoglu, Small interfering RNA-mediated xCT silencing in gliomas inhibits neurodegeneration and alleviates brain edema, *Nat. Med.* 14 (2008) 629–632.
- [21] D.N. Simopoulos, S.J. Gibbons, J. Malysz, J.H. Szurszewski, G. Farrugia, E.L. Ritman, R.B. Moreland, A. Nehra, Corporeal structural and vascular micro architecture with X-ray micro computerized tomography in normal and diabetic rabbits: histopathological correlation, *J. Urol.* 165 (2001) 1776–1782.
- [22] W. Stiller, M. Kobayashi, K. Koike, U. Stampfl, G.M. Richter, W. Semmler, F. Kiessling, Initial experience with a novel low-dose micro-CT system, *Fortschr. Roentgenstr.* 179 (2007) 669–675.
- [23] G.H. Vince, M. Bendszus, T. Schweitzer, R.H. Goldbrunner, S. Hildebrandt, J. Tilgner, R. Klein, L. Solymosi, J.C. Tonn, K. Roosen, Spontaneous regression of experimental gliomas—an immunohistochemical and MRI study of the C6 glioma spheroid implantation model, *Exp. Neurol.* 190 (2004) 478–485.
- [24] A. von Deimling, D.N. Louis, O.D. Wiestler, Molecular pathways in the formation of gliomas, *Glia* 15 (1995) 328–338.